Dynamic Rate Adaptation Based on Multidimensional Multicode DS-CDMA in Cellular Wireless Networks

Dong In Kim, *Senior Member, IEEE*, Ekram Hossain, *Member, IEEE*, and Vijay K. Bhargava, *Fellow, IEEE*

***Abstract*—Dynamic rate adaptation for uplink data transmission in a cellular multidimensional multicode (MDMC) direct-sequence code-division multiple-access packet data network is modeled and analyzed in this paper. An analytical framework is developed to evaluate the performances of radio link level dynamic rate adaptation schemes under multipath fading and log-normal shadowing. The radio link level throughput under *optimal* dynamic rate adaptation (having exponential computational complexity) and different heuristic-based suboptimal rate adaptation schemes can be assessed under the presented analytical framework. The performance of MDMC signaling is compared with that of the single-code variable spreading factor (VSF) signaling. To this end, based on an equilibrium point analysis of the system in steady-state, a base station-assisted and mobile-controlled dynamic rate adaptation scheme is presented.**

***Index Terms*—Base station (BS)-assisted mobile-controlled algorithm, dynamic rate adaptation, joint multicell rate adaptation, multidimensional multicode (MDMC) signaling.**

I. Introduction

WIDEBAND code-division multiple-access (WCDMA) systems (e.g., ETSI WCDMA, cdma2000) will be the major radio transmission technologies for IMT-2000. These systems have intrinsic support for adaptive packet data access on a frame-by-frame basis, which is achievable through variable-rate data transmission. Multicode (MC) transmission [1] and single-code transmission with variable spreading factor (VSF) [2] are two different ways of implementing varible-rate transmission. In an MC WCDMA system, each spreading code carries a basic rate, and m codes are provided in parallel to enable a user to transmit at m times the basic rate capability. Therefore, the number of active channels m is variable during the call, while the spreading gain on each channel is generally kept fixed (although a finer rate quantization can be achieved by allowing variable spreading gain in each channel). In the case of single-code transmission with variable spreading gain, each user transmits using only one code channel and the spreading gain varies inversely with the transmission rate. Some minimum required spreading gain may limit the highest achievable transmission rate in a single-code VSF system.

Since high-rate services in an MC WCDMA system can only be implemented using a large number of parallel channels, it leads to complex transmitter and RAKE receiver implementations [3]. In addition, for uplink transmission, conventional MC transmission may incur high power consumption in the mobile terminal. This is due to the higher requirements on the linearity of the mobile terminal transmitter power amplifier resulting from the larger envelope variations in the transmitted signal [3]. MDMC signaling [4], which generally uses a fixed number of codes for transmission, can overcome some of these limitations.

In MDMC signaling, transmission is based on multiple orthogonal parallel channels and the effect of self-interference among the parallel channels (which becomes more severe as the number of channels increases, especially in multipath fading environments) is minimized. In addition, a constant envelope signal is generated using precoding channels.

Dynamic rate adaptation in a WCDMA system can increase the statistical multiplexing gain with a consequent increase in instantaneous system throughput. Therefore, it can play a role which is analogous to that of dynamic link adaptation in narrowband systems (e.g., enhanced data for GSM evolution (EDGE) [5]). The aim is to maximize the overall network throughput which is constrained by channel fading, interference, and noise. Fast and simple algorithms for dynamic rate adaptation based on the channel status (which is a function of channel load and error characteristics) need to be developed for cellular WCDMA systems.

The issue of finding fast and efficient suboptimal solutions of the dynamic rate-allocation problem was addressed in [6]. Two interference-based dynamic rate-allocation procedures for uplink packet data transmission in a single-code VSF WCDMA system were proposed and analyzed therein. This paper addresses the problem of modeling and analysis of dynamic rate adaptation in MDMC direct-sequence code-division multiple access (DS-CDMA) cellular wireless networks where the dynamic rate adaptation is performed considering only a single class of users with similar quality of service (QoS) requirements, while trying to maximize the radio link level throughput. An analytical framework is developed to evaluate radio link level throughput under dynamic rate adpatation in cellular MDMC and VSF DS-CDMA networks for two automatic repeat request (ARQ)-based radio link level error control alternatives, namely, Selective Repeat (SR) and Go-Back-m

Paper approved by E. Ayanoglu, the Editor for Communication Theory and Coding Application of the IEEE Communications Society. Manuscript received October 22, 2000; revised January 25, 2002. This work was supported in part by the Brain Korea 21 Project and in part by the Natural Sciences and Engineering Research Council (NSERC) of Canada.

D. I. Kim was with the University of Seoul, Seoul, Korea. He is now with the School of Engineering Science, Simon Fraser University, Burnaby, BC V5A 1S6, Canada (e-mail: dikim@sfu.ca).

E. Hossain is with the Department of Electrical and Computer Engineering, University of Manitoba, Winnipeg, MB R3T 5V6, Canada (e-mail: ekram@ee.umanitoba.ca).

V. K. Bhargava is with the Department of Electrical and Computer Engineering, University of Victoria, Victoria, BC V8W 3P6, Canada (e-mail: bhargava@ece.uvic.ca).

Digital Object Identifier 10.1109/TCOMM.2003.809263

(GBm). Radio link level throughput under optimal[1] dynamic rate adaptation can be also assessed under the presented analytical framework. To this end, based on an equilibrium point analysis of the system in steady state, a base station (BS)-assisted and mobile-controlled dynamic rate adaptation procedure is proposed and analyzed.

The rest of the paper is organized as follows. The system model, which describes the MDMC signaling and the problem of optimal rate allocation is presented in Section II. The analysis of signal-to-interference-plus-noise ratio (SINR) in a single cell with MDMC signaling in the presence of multipath fading and log-normal shadowing is presented in Section III. Two SINR models for performance evaluation of dynamic rate adaptation in a multicell DS-CDMA environment are presented in Section IV. Several heuristic-based dynamic rate adaptation algorithms are presented in Section V. In Section VI, the radio link level throughput with MDMC signaling under the proposed rate adaptation algorithms is evaluated for the two radio link level error control alternatives, namely, SR and GBm. A BS-assisted and mobile-controlled dynamic rate selection procedure is presented in Section VII. Conclusions are stated in Section VIII.

II. System Model

A. Variable Rate Transmission and Optimal Rate Allocation

A time-framed system is considered here, in which the frame duration is fixed. Depending on the rate allocation, however, a mobile station can transmit a variable number of fixed-length radio link control (RLC)/medium access control (MAC) layer frames, which are derived from the segmentation of variable-length Internet protocol (IP) packets, within one frame time. Let the length of a frame be denoted by T_f and the transmission rates be selected from the set of rates $\{v_0, v_1, \ldots, v_\varphi\}$ (where $v_m = mv_1$, $m = 0, 1, \ldots, \varphi$) such that the throughput during a frame time is maximized. The throughput is a function of the actual traffic load and the channel condition. If it is assumed that only one frame (of fixed length of N_f bits) corresponding to the smallest (basic) rate v_1 can be transmitted during a frame time, then for rate v_m, m frames can be transmitted during the a frame time.[2]

We refer to Table I for the list of key mathematical notations used in this paper.

TABLE I
List of Key Notations

g_j, $j = 1, \cdots, J$	Number of mobiles in cell j
g	Number of mobiles per cell for uniform traffic load
$m_i^{(j)}$	Transmission rate for ith mobile in cell j
$P_{b,i}^{(j)}$	Power allocated to ith mobile in cell j for the basic rate v_1
$\rho_j(j', k)$	L-path fading for the link between $(BS)_j$ and kth mobile in cell j'
$L_j(j', k)$	Long-term fading for the link between $(BS)_j$ and kth mobile in cell j'
$m_i^{(j)} \times P_{b,i}^{(j)}$	Total power allocated to ith mobile in cell j
P_b	Received signal power at BS for rate v_1
$\eta_{j'/j}(k)$	Other-cell interference factor in cell j for transmission from kth mobile in cell j'
$(SINR)_{o,i}^{(j)}$	Output SINR correponding to ith mobile in cell j
$\bar{\eta}_j$	Average value of other-cell interference factor in cell j
$p_{b,m}$	Probability of bit error for a user with rate v_m
$p_{c,m}$	Probability of correct frame reception for a user transmitting at rate v_m
β	Radio link level throughput, frames/frame−time
p_s	Probability of rate increase (upon successful transmission)
p_f	Probability of rate decrease (upon transmission failure)

The problem of finding the optimal rate allocation $\mathbf{n}$ under such variable rate transmission scenario can be described as

$$\max_{\mathbf{n}} \beta(\mathbf{n}) \qquad \text{subject to} \sum_{m=0}^{\varphi} n_m = g \tag{1}$$

where $\mathbf{n} \triangleq (n_0, n_1, \ldots, n_\varphi)$, n_m denotes the number of users with rate $v_m (m = 0, 1, \ldots, \varphi)$, and g is the total number of active users during a frame time in a tagged cell. Here, the throughput β in a tagged cell can be expressed by

$$\beta(\mathbf{n}) = \sum_{m=1}^{\varphi} m n_m p_{c,m} \qquad \text{frames/frame time} \tag{2}$$

where the probability of correct frame reception $p_{c,m}$ at rate v_m depends on the channel interference and fading conditions, and on the error-control scheme employed.

If two or more cells (say, N_c cells) are jointly involved in the rate adaptation, the optimal rate-allocation problem in (1) can be restated as

$$\max_{(\mathbf{n}_1, \ldots, \mathbf{n}_{N_c})} \beta(\mathbf{n}_1, \ldots, \mathbf{n}_{N_c})$$
$$\text{subject to} \sum_{m=0}^{\varphi} n_{m,j} = g_j; \qquad j = 1, \ldots, N_c \tag{3}$$

where $\mathbf{n}_j \triangleq (n_{0,j}, n_{1,j}, \ldots, n_{\varphi,j})$ corresponds to the jth tagged cell. In this case, for a total of J cells, the other-cell interference is caused in part by the $(N_c - 1)$ cells with actual traffic loads $\{g_j\}$, and in part by the rest of the cells (i.e., $(J - N_c)$ cells).

[1]Maximization of radio link level throughput is the optimality criterion in this case.

[2]For the rest of the paper it is assumed that $v_m = mv_1$ so that the normalized value of v_m with respect to the basic rate v_1 is m.

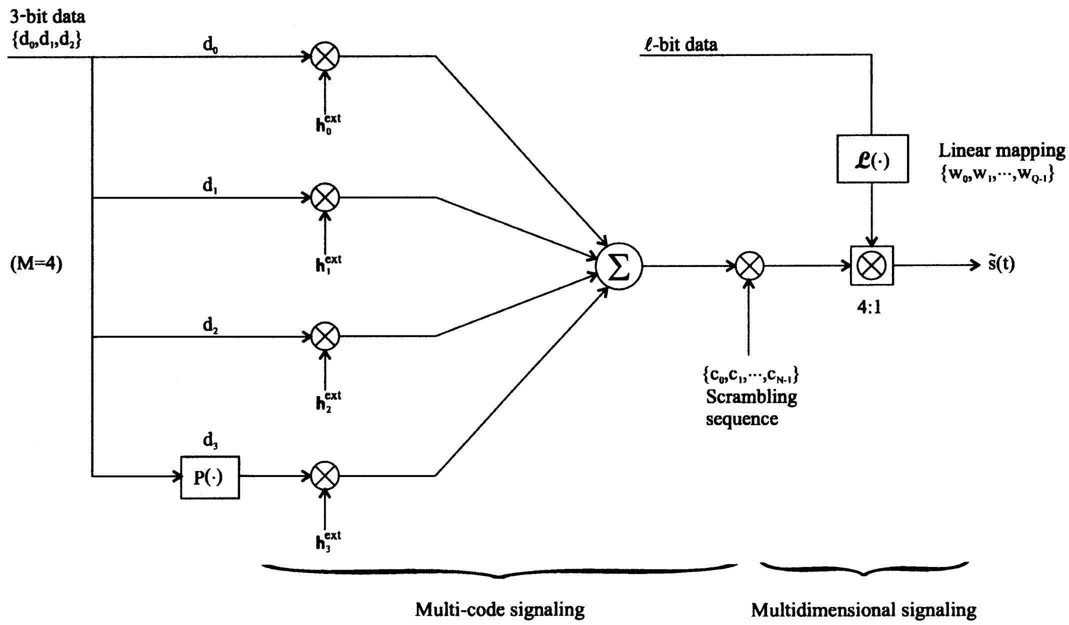

Fig. 1. Transmitter for MDMC signal when $M = 4$.

Interferences from these $(J - N_c)$ cells can be characterized by a mean-sense approximation [6]. With joint multicell rate adaptation, the sum of the throughtputs in N_c cells is

$$\beta(\mathbf{n}_1, \ldots, \mathbf{n}_{N_c}) = \sum_{j=1}^{N_c} \sum_{m=1}^{\varphi} m n_{m,j} p_{c,m}^{(j)} \quad \text{frames/frame time.} \tag{4}$$

Thus, for joint multicell rate adaptation, the effects of the above two types of other-cell interference should be reflected in the probability $p_{c,m}^{(j)}$.

B. MDMC Signaling for Variable Rate Transmission

For variable rate transmission, MDMC DS-CDMA signaling is employed, which was proposed in [4], to provide transmission rates up to $\varphi = 8$ using M (e.g., $M = 4$)-parallel code channels, while maintaining a constant spreading factor N per symbol. The MC signaling, considered for high-rate transmissions in WCDMA uplink [7], uses dual binary phase-shift keying (BPSK) for data modulation and quaternary phase-shift keying (QPSK) for spreading. The MDMC signaling introduces additional Q-ary orthogonal modulation for each subset of $I\,(\leq\ M)$-parallel code channels with $Q \triangleq N/M$, which results in *bi-orthogonal* signaling and carries a maximum of $(M + M/I \log_2 Q)$-bit information per symbol. The MDMC signaling increases the data rate compared to the MC signaling by exploiting the user-specific signature sequence as part of the data modulation. Here, the resulting user-specific signature sequence is concatenated by the Q-ary modulating sequence that carries the maximum $\log_2 Q$-bit information [4].

The main difference between the MDMC DS-CDMA and the parallel-combinatorial DS-CDMA proposed in [8] is that the design of the concatenated signature sequence can be performed in many different ways for the MDMC signaling. For instance, when M-parallel MC signaling is considered, the Q-ary modulating sequence can be inserted into any subset of $I\,(\leq M)$-parallel MC signaling, resulting in a large degree of freedom to increase the data rate as far as it is allowed. For example, if $I = 1$, additional data of $M \log_2 Q$ bits per symbol can be sent, which far exceeds M bits per symbol obtainable using the MC signaling.

Note that BPSK DS-CDMA is used for $m = 1$ and dual BPSK DS-CDMA is adopted when $m = 2$. For $3 \leq m \leq \varphi = 8$, the MDMC BPSK DS-CDMA signal $s(t)$ is constructed as follows:

$$\tilde{s}(t) = \sum_{q=0}^{Q-1} \sum_{n=0}^{M-1} \sum_{i=0}^{M-1} d_i h_{i,n}\, w_q\, c_{qM+n}\, p(t - (qM + n)T_c) \tag{5}$$

where $s(t) = \Re\{\sqrt{2P}\,\tilde{s}(t) \exp(j\omega_c t)\}$, P is the signal power per code channel, ω_c is the carrier frequency, the spreading factor N per symbol is equal to QM, $\{d_i\}$ denote M-parallel binary data, $H_M = [h_{i,n}]$ is the Hadamard matrix of elements ± 1, $(w_0, w_1, \ldots, w_{Q-1})$ is a modulating sequence to be selected by l-bit binary data ($l \leq \log_2 Q$) from the subset of 2^l row vectors in any orthogonal matrix of size Q-by-Q (e.g., H_Q), $\{c_{qM+n}\}$ is the user-specific signature sequence that results in the concatenated signature sequence $\{w_q c_{qM+n}\}$ due to the 2^l-ary orthogonal modulation, and $p(t)$ is a rectangular chip pulse of unit magnitude, occupied in [0, T_c).

A one-bit precoding is used for a constant envelope MC signal of magnitude $\sqrt{M}$ to avoid nonlinear distortions in uplink transmission when $M = 4$, and then $(3 + l)$ bits can be conveyed via $s(t)$. If we choose $Q = 32$ and $N = QM = 128$ per symbol, $l \leq \log_2 Q = 5$ is selected to send the data of $3 \leq m \leq \varphi = 8$ bits per symbol. To illustrate, Fig. 1 shows the transmitter to generate the MDMC signal $\tilde{s}(t)$ when $M = 4$ [4].

Note that the MDMC signaling can be easily applied to both the IMT-2000 and IS-95 uplink transmissions using only BPSK modulation with QPSK spreading.

C. Dynamic Rate Allocation and Radio Link Level Error Recovery

Each user can transmit the variable data of $1 \leq m \leq \varphi = 8$ bits using the above signals over a symbol time $T = NT_c$, while an optimum rate combination during a frame time may be determined using actual traffic load[3] or an estimate of the traffic load, the location of the mobiles, the interference generated by each mobile, and the transmit power levels at the different mobiles (as will be described later in this paper). The dynamic rate allocation is then broadcast by the BS using a control channel.

Either SR- or GBm-based error control proposed in [6] can be adopted for radio link level error recovery. In case of SR-based error control, each frame (of length N_f bits) transmitted during a frame time is treated independently so that only the frames involved in errors will be retransmitted. The GBm scheme assumes a whole frame decoding rather than an individual frame decoding within a frame time. That is, the m frames transmitted during a frame time (with transmission rate v_m) are treated as one single frame of length mN_f bits. Therefore, when the whole frame is declared to have failed after decoding, all the m frames during that frame time will be retransmitted.

III. Characterization of Total Multiple Access Interference (MAI) in a Cell Under MDMC Signaling in Fading Channels

Suppose that the kth mobile in a desired cell $j = 1, 2, \ldots, J$, transmits its signal at a specific rate $m_k^{(j)} \in \{0, 1, \ldots, \varphi\}$ according to the optimal rate allocation $\mathbf{n}$ as in (1). Then, the received signal with only the in-cell interference is modeled as

$$r(t) = \sum_{k=1}^{g_j} \sum_{l=1}^{L} \beta_{k,l}^{(j)} s_k^{(j)}(t - \tau_{k,l}^{(j)}) + n(t) \tag{6}$$

where the index j represents the tagged cell, $\beta_{k,l}^{(j)}$ and $\tau_{k,l}^{(j)}$ are the channel gain and delay for the kth user in cell j and lth path, and $n(t)$ is the additive white Gaussian noise (AWGN) with two-sided power spectral density (PSD) $N_o/2$. Here, $s_k^{(j)}(t)$ is obtained from $s(t)$ using: 1) $m_k^{(j)} = 1$ for the BPSK DS-CDMA with $\tilde{s}(t) = \sum_{n=0}^{N-1} d_0 c_n p(t - nT_c)$; 2) $m_k^{(j)} = 2$ for the dual BPSK DS-CDMA with $\tilde{s}(t) = \sum_{n=0}^{N-1} [d_0 + jd_1] c_n p(t - nT_c)$; 3) $3 \leq m_k^{(j)} \leq \varphi = 8$ from $\tilde{s}(t)$ in (5), where d_i, c_n, $(w_0, w_1, \ldots, w_{Q-1})$, and P are replaced by $d_{i,k}^{(j)}$, $c_{n,k}^{(j)}$, $(w_{0,k}^{(j)}, w_{1,k}^{(j)}, \ldots, w_{Q-1,k}^{(j)})$, and $P_k^{(j)}$.

For the variable-rate transmission, the transmit signal power $P_k^{(j)}$ per code channel for the kth user in cell j can be written as

$$P_k^{(j)} = \frac{m_k^{(j)} P_{b,k}^{(j)}}{\kappa_{m_k^{(j)}}} \tag{7}$$

where $P_{b,k}^{(j)}$ is the transmit power at the basic rate and $mP_{b,k}^{(j)}$ is the transmit power with rate v_m, $\kappa_m = m$ if $m = 1, 2$ (single/dual channels) and $\kappa_m = 4$ for $3 \leq m \leq \varphi = 8$ due to $M(=4)$-parallel code channels.

Assume that the signal from the ith mobile $s_i^{(j)}(t)$ is desired, and the (normalized) correlated output corresponding to the lth path at the BS j, $(\mathrm{BS})_j$ is given by

$$\begin{aligned} Z_{i,l}^{(j)} =& \frac{1}{T\sqrt{\kappa_{m_i^{(j)}} P_i^{(j)}}} \int_{\tau_{i,l}^{(j)}}^{T+\tau_{i,l}^{(j)}} r(t) s_i^{(j)}(t - \tau_{i,l}^{(j)})\, dt \\ =& \beta_{i,l}^{(j)} \sqrt{m_i^{(j)} P_{b,i}^{(j)}} + \mathrm{MAI}_{i,l}^{(j)} + N_{i,l}^{(j)} \end{aligned} \tag{8}$$

where $N_{i,l}^{(j)}$ is zero-mean Gaussian noise with variance $N_o/(2T)$, and $\mathrm{MAI}_{i,l}^{(j)}$ is given by (9). After a few steps, the cross-correlation function $\lambda_{k,l'}^{(j)}$ can be defined by (10), where $*$ denotes the complex conjugate and $\theta_{k,l',l}^{(j)} = -\omega_c \left(\tau_{k,l'}^{(j)} - \tau_{i,l}^{(j)}\right)$

$$\begin{aligned} \mathrm{MAI}_{i,l}^{(j)} =& \sum_{\substack{k=1 \\ k \neq i}}^{gj} \sum_{l'=1}^{L} \beta_{k,l'}^{(j)} \sqrt{m_k^{(j)} P_{b,k}^{(j)}} \lambda_{k,l'}^{(j)} \\ &+ \sum_{\substack{l'=1 \\ l' \neq l}}^{L} \beta_{i,l'}^{(j)} \sqrt{m_i^{(j)} P_{b,i}^{(j)}} \lambda_{k,l'}^{(j)}. \end{aligned} \tag{9}$$

$$\begin{aligned} \lambda_{k,l'}^{(j)} =& T^{-1} \int_{\tau_{i,l}^{(j)}}^{T+\tau_{i,l}^{(j)}} \\ & \Re\left\{ \frac{\tilde{s}_k^{(j)}(t - \tau_{k,l'}^{(j)})}{\sqrt{k_{m_k}^{(j)}}} \cdot \frac{\tilde{s}_i^{(j)*}(t - \tau_{i,l}^{(j)})}{\sqrt{k_{m_i}^{(j)}}} \exp(j\theta_{k,l',l}^{(j)}) \right\} dt. \end{aligned} \tag{10}$$

Since $\tilde{s}_k^{(j)}(t)$ is a constant envelope signal of magnitude $\sqrt{\kappa_{m_k^{(j)}}}$ due to one-bit precoding, $\lambda_{k,l'}^{(j)}$ is equivalent to

$$\lambda_{k,l'}^{(j)} \equiv \langle c(t),\, \hat{c}(t - \tau_{k,l',l}^{(j)}) \rangle \cdot \cos\left(\theta_{k,l',l}^{(j)}\right) \tag{11}$$

where $\langle \cdot, \cdot \rangle$ denotes the temporal average operation, $c(t)$ and $\hat{c}(t)$ represent two uncorrelated, binary code sequences of duration T_c, and $\tau_{k,l',l}^{(j)} = \tau_{k,l'}^{(j)} - \tau_{i,l}^{(j)}$. For random binary sequences,[4] it can be easily shown [9] that

$$\mathbf{var}[\lambda_{k,l'}^{(j)}] = (3N)^{-1}. \tag{12}$$

Then, the RAKE combiner's output is defined by $Z_i^{(j)} = \sum_{l=1}^{L} \beta_{i,l}^{(j)} Z_{i,l}^{(j)}$, where the (output) SINR $(\mathrm{SINR})_{o,i,l}^{(j)}$ for the lth path is derived as in (13) at the bottom of the next page, where $\mathbf{E}[x]$ and $\mathbf{var}[x]$ denote the expectation and variance of x, respectively.

Since the second term in the denominator of (13) can be often neglected, a conservative estimate of the RAKE-combined output SINR, $(\mathrm{SINR})_{o,i}^{(j)} = \sum_{l=1}^{L} (\mathrm{SINR})_{o,i,l}^{(j)}$, can be expressed as in (14) at the bottom of the next page, where $\sum_{l'=1}^{L} \left(\beta_{k,l'}^{(j)}\right)^2 \triangleq \rho_j(j,k) L_j(j,k)$, and $\rho_j(j,k)$ and $L_j(j,k)$ represents the channel gain between $(\mathrm{BS})_j$ and the kth user in cell j due to short-term and long-term fading, respectively.

[3]A mobile may inform the BS that a frame is ready to be transmitted by using subrate control channel.

[4]In fact, user-specific long signature sequences are used in the uplink to maximize the MAI averaging effect.

With uplink power control, the received signal power at basic rate can be written as

$$P_b = \rho_j(j,k)L_j(j,k)P_{b,k}^{(j)} \quad \text{for } k = 1,2,\ldots,g_j \text{ and } j = 1,2,\ldots,J. \tag{15}$$

Therefore, the RAKE-combined output SINR in (14) can be formulated as

$$(\mathrm{SINR})_{o,i}^{(j)} = m_i^{(j)}\left[\frac{1}{3N}\sum_{k=1}^{g_j} m_k^{(j)} + \left(\frac{2E_b}{N_o}\right)^{-1}\right]^{-1} \tag{16}$$

where $E_b = P_bT$ is the received bit energy.

IV. SINR Modeling and Dynamic Rate Adaptation

A. SINR Model Based on Mean-Sense Approximation of Other-Cell Interference (SINR Model-1)

Assume that the traffic load $g_j(j = 1,2,\ldots,J)$ in all the cells is given by $g_j = g$ transmission attempts per frame time and that the impact of other-cell interference in the target cell (which is caused by a large number of neighboring cells) can be characterized in a mean sense. This assumption can be relaxed to the case where the traffic load in different cells vary, but the average load over all cells is kept fixed to some value (say, g).[5] Then, the expression for the RAKE-combined output SINR in (16) can be modified by taking the other-cell interference into account as follows [10]:

$$(\mathrm{SINR})_{o,i}^{(j)} = m_i^{(j)}\left[\frac{1}{3N}\left(\sum_{k=1}^{g_j} m_k^{(j)}\right)(1+\bar{\eta}_j) + \left(\frac{2E_b}{N_o}\right)^{-1}\right]^{-1} \tag{17}$$

where the average other-cell interference factor in the tagged cell j is defined by [6]

$$\bar{\eta}_j = \sum_{j'\neq j}\left(\frac{1}{g_{j'}}\sum_{k=1}^{g_{j'}} \eta_{j'/j}(k)\right). \tag{18}$$

Here, the other-cell interference factor $\eta_{j'/j}(k)$ is defined by

$$\eta_{j'/j}(k) \triangleq \frac{\rho_j(j',k)L_j(j',k)}{\rho_{j'}(j',k)L_{j'}(j',k)} \tag{19}$$

in which the short-term fading (i.e., Rayleigh fading) is given by $\rho_j(j',k) = \sum_{l=1}^{L} a_{j,k(j'),l}^2$ with $a_{j,k(j'),l}$ being the lth path gain between $(\mathrm{BS})_j$ and the kth mobile in cell j', and the long-term fading $L_j(j',k)$ for the same link is modeled as

$$L_j(j',k) = r_{j,k(j')}^{-\delta}\cdot 10^{\xi_{j,k(j')}/10} \tag{20}$$

assuming that the signal between $(\mathrm{BS})_j$ and the kth mobile in cell j' is attenuated by the δth power of the distance $r_{j,k(j')}$ and log-normal shadowing (ξ is a zero-mean normal variate with standard deviation σ).

The impact of other-cell interference is taken into consideration in an average sense (by introducing the average other-cell interference factor $\bar{\eta}_j$) in the above SINR formulation. Since the interference and fading conditions are highly dynamic (due to user location and mobility patterns), the SINR corresponding to a mobile transmitter would vary from one snapshot to another, depending on the channel matrix, and it would vary from cell to cell even in the presence of uniform traffic load. Therefore, in a multicell environment, an average-sense approach enables us to estimate the system performance in a cell without taking user location and the micromobility issues explicitly into consideration.

The impact of other-cell interference becomes more significant with increasing sum rate $\sum_{k=1}^{g_j} m_k^{(j)}$ and as a result, the radio link level throughput will decrease. This implies that the above SINR modeling provides a conservative estimate on the rate allocation when the sum rate becomes large in a cell. On the other hand, if the sum rate is relatively small, then the rate allocation is somewhat optimistic, due to the reduced impact of other-cell interference.

In the case of VSF signaling, the expression for SINR under mean-sense approximation of the other-cell interference is given as follows [6]:

$$(\mathrm{SINR})_{o,i}^{(j)} = \left[\frac{1}{3N}\left(\sum_{k=1}^{g_j} m_k^{(j)}\right)(1+\bar{\eta}_j) + \left(\frac{2E_b}{N_o}\right)^{-1}\right]^{-1}. \tag{21}$$

B. SINR Model Based on Mean-Sense Approximation Along With Exact Calculation of Other-Cell Interference (SINR Model-2)

This model considers explicitly the other-cell interference factors corresponding to the mobiles confined only to a small subset of N_c (e.g., $N_c = 2,3$) cells (rather than the entire set of J cells). That is, two types of other-cell interference are considered: interference that results from the $(N_c - 1)$ cells with actual traffic loads $\{g_j\}$ and interference from the other $(J - N_c)$ cells

[5]This can be achieved through the radio network controller (RNC) in a WCDMA network.

$$(\mathrm{SINR})_{o,i,l}^{(j)} = \frac{\mathbf{E}^2\left[\beta_{i,l}^{(j)}Z_{i,l}^{(j)}|\{\beta_{k,l}^{(j)}\}\right]}{\mathbf{var}[\beta_{i,l}^{(j)}Z_{i,l}^{(j)}|\{\beta_{k,l}^{(j)}\}]} = \frac{\left(\beta_{i,l}^{(j)}\right)^2 m_i^{(j)}P_{b,i}^{(j)}}{\frac{1}{(3N)}\sum_{k=l}^{gj}\sum_{l'=1}^{L}\left(\beta_{k,l'}^{i}(j)\right)^2 m_k^{(j)}P_{b,k}^{(j)} - \frac{1}{(3N)}\left(\beta_{i,l}^{(j)}\right)^2 m_i^{(j)}P_{b,i}^{(j)} + \frac{N_0}{(2T)}} \tag{13}$$

$$(\mathrm{SINR})_{o,i}^{(j)} = \frac{\rho_j(j,i)L_j(j,i)m_i^{(j)}P_{b,i}^{(j)}}{\frac{1}{(3N)}\sum_{k=1}^{gj}\rho_j(j,k)L_j(j,k)m_k^{(j)}P_{b,k}^{(j)} + \frac{N_0}{(2T)}} \tag{14}$$

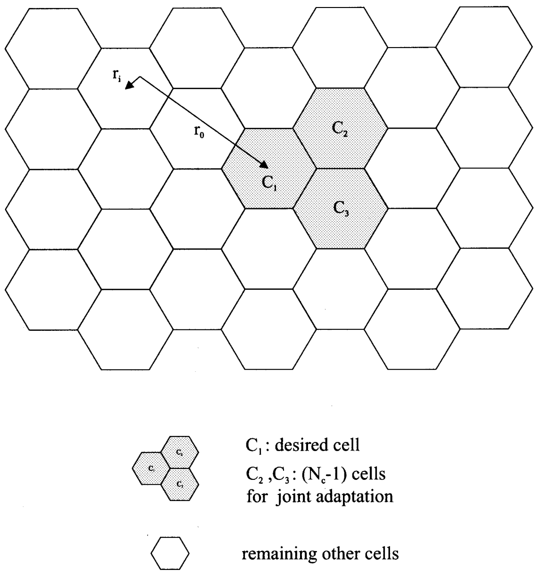

Fig. 2. Hexagonal cell layout for joint N_c-cell rate adaptation.

(as shown in Fig. 2). Interference in the tagged cell j due to the other $(J-N_c)$ cells is evaluated in a mean sense, and the mean-sense interference factor is given by

$$\hat{\eta}_j = \sum_{j'>N_c} \left(\frac{1}{g_{j'}} \sum_{k=1}^{g_{j'}} \eta_{j'/j}(k) \right). \tag{22}$$

All N_c cells considered here are assumed to be adjacent to each other in a hexagonal cell layout. Then, the RAKE-combined output SINR in (17) can be formulated as in (23). With this SINR modeling, the expression for SINR in the case of VSF signaling is given by (24) [6].

$$(\mathrm{SINR})_{o,i}^{(j)} = m_i^{(j)} \left[\frac{1}{3N} \left(\sum_{k=1}^{gj} m_k^{(j)} \right) (1+\hat{\eta}_j) + \frac{1}{3N} \sum_{\substack{j'=1 \\ j'\neq j}}^{N_c} \sum_{k=1}^{g_{j'}} m_k^{(j')} \eta_{j'/j}(k) + \left(\frac{2E_b}{N_0} \right)^{-1} \right]^{-1}. \tag{23}$$

$$(\mathrm{SINR})_{o,i}^{(j)} = \left[\frac{1}{3N} \left(\sum_{k=1}^{gj} m_k^{(j)} \right) (1+\hat{\eta}_j) + \frac{1}{3N} \sum_{\substack{j'=1 \\ j'\neq j}}^{N_c} \sum_{k=1}^{g_{j'}} m_k^{(j')} \eta_{j'/j}(k) + \left(\frac{2E_b}{N_0} \right)^{-1} \right]^{-1}. \tag{24}$$

In general, mobiles in the different cells experience different patterns of other-cell interference. With SINR Model-2, the interference due to each individual mobile within a group of neighboring cells can be taken into account explicitly, and therefore, by performing joint multicell rate adaptation based on SINR Model-2, the effect of other-cell interference may be minimized in the involved cells.

C. Optimal Dynamic Rate Adaptation

During dynamic rate adaptation, if higher transmission rates are allocated to mobiles in a cell, it causes the other-cell interference to increase which, in turn, may reduce the throughput in other cells. Therefore, for a multicell system (with J cells), the optimal rate allocation over all the cells could be found that minimizes the other-cell interference and maximizes the total system throughput

$$\text{choose } m_i^{(j)} \text{ for } i, j \text{ subject to maximizing } \beta. \tag{25}$$

This optimal rate allocation in (25) can be determined by an exhaustive search (having exponential computational complexity) to find the rate combinations $\{m_i^{(j)} \mid i = 1,2,\ldots,g_j,\ j = 1,2,\ldots,J\}$ that maximize system throughput. To avoid this huge computational complexity, low-complexity suboptimal dynamic rate adaptation schemes are required. Several heuristic-based suboptimal rate adaptation schemes will be presented later in this paper.

Again, a SINR model that involves all the other-cell interference factors $\{\eta_{j'/j}(k)\}$ ($\forall k, j' \neq j,\ k = 1,\ldots,g_{j'}$ and $j' = 1,\ldots,J$) would incur significant complexity in implementation of any dynamic rate adaptation scheme.

D. Dynamic Rate Adaptation Based on SINR Model-1

The mean-sense approach avoids the above implementation complexity by considering the other-cell interference factors $\{\eta_{j'/j}(k)\}$ in an average sense while determining the rate allocation for the mobiles in the tagged cell j. Therefore, SINR Model-1 basically lends itself to simple single-cell dynamic rate adaptation. In this case, a single other-cell interference factor for each cell (i.e., $\bar{\eta}_j$ for cell j, which can be estimated by the RNC) can be used by the corresponding BS to determine the rate allocation among the different mobiles in that cell.

With SINR Model-1, some heuristic-based rate allocation can be used to allocate rates among mobiles in a cell that will maximize the throughput so that the complexity of an exhaustive search to determine the rate allocation can be avoided. Since the spatial distribution of the mobiles is not taken explicitly into account, and since the rate allocation tries to optimize the radio link level throughput, the performances of the optimal and the suboptimal schemes would be *almost* the same.

E. Dynamic Rate Adaptation Based on SINR Model-2

The key to the efficient dynamic rate adaptation in a cellular WCDMA system lies in the intelligent management of in-cell and other-cell interferences. Since the SINR Model-1 above takes into account the other-cell interference in an average sense, dynamic rate adaptation using SINR Model-1 is unable to take into account and effectively control the other-cell interference, which is impacted largely by the spatial distribution of the mobiles. On the other hand, SINR Model-2 which takes the other-cell interference caused by (N_c-1) cells explicitly into consideration, lends itself to joint multicell rate adaptation over N_c cells.

By joint multicell rate adaptation, the impact of $\{\eta_{j'/j}(k) \mid j' \neq j = 1,2,\ldots,N_c\}$ in the N_c adjacent cells involved can be minimized so that the rate allocation is optimized to produce the maximum throughput $\beta(\mathbf{n}_1, \ldots, \mathbf{n}_{N_c})$ in (3). Note that, with $N_c = J$ in this SINR model, the optimal rate allocation over all the J cells could be determined using an exhaustive search among all possible rate allocations to all the mobiles in these cells.

Since it requires estimation of, on the average, $1/N_c \sum_{j=1}^{N_c}$ interference factors per cell, the implementation complexity of the adaptation scheme increases with increasing N_c. Again, with $N_c < J$, to reduce the computational complexity, heuristic-based suboptimal rate-allocation schemes can be used (instead of exhaustive search-based optimal rate allocation) within these N_c cells.

Note that, the issue of SINR modeling for dynamic rate adaptation in a cellular DS-CDMA network is decoupled from the issue of dynamic rate adaptation in this paper. For both the SINR models described above, optimal[6] and suboptimal (e.g., heuristic-based) rate allocations can be determined. The optimal rate allocation to all the mobiles in all the J cells can be determined using SINR Model-2 with $N_c = J$ only.

V. Heuristic-Based Rate Adaptation Algorithms

A. Channel Gain-Based Dynamic Rate Adaptation

In this case, the maximum allowable transmission rates are allocated to the mobiles with higher channel gains. Mobiles located near the cell boundary would presumably have lower channel gains, and therefore, allocating higher transmission rates to these mobiles would increase interference to adjacent cells. With uplink power control the transmit power levels $\{P_{b,k}^{(j)}\}$ are inversely proportional to the channel gains as in (15).

Under single-cell rate adaptation, the rate allocation $\{m_k^{(j)}\}$ in the tagged cell j can be performed by using the channel gains $\{\rho_j(j,k)L_j(j,k)\}$ as follows. Allocate the maximum allowable rate to the mobiles in an increasing order of the transmit power levels (or decreasing order of channel gains) while trying to maximize $\beta(\mathbf{n})$ in (2) using SINR Model-1.

The joint multicell rate allocation $\{m_k^{(j)} \,|\, j = 1, 2, \ldots, N_c\}$ over N_c cells can be performed similarly to the single-cell rate allocation by measuring the transmit power levels $\{P_{b,k}^{(j)} \,|\, j = 1, 2, \ldots, N_c\}$, where the maximum allowable rate is allocated to the mobiles in an increasing order of the transmit power levels, while trying to maximize $\beta(\mathbf{n}_1, \ldots, \mathbf{n}_{N_c})$ using SINR Model-2.

Note that, when the rate zero is allocated to the kth mobile in cell j', $m_k^{(j')} \times \eta_{j'/j}(k) = 0$. Therefore, by restricting the rate allocation to a few mobiles with the most favorable channel conditions, the impact of other-cell interference can be minimized.

For the above rate-allocation procedure, the rate allocation is restricted only to two possible rates: φ and m $(1 \le m < \varphi)$. Therefore, the rate allocation leads to some extreme rate distribution while maximizing the total system throughput.

B. Peak Interference-Based Dynamic Rate Adaptation

The idea behind this suboptimal scheme is to minimize the peak interference to other adjacent cells by allocating lower transmission rates to mobiles which may generate high interference to other cells. Especially, high-rate transmission from a mobile located near the cell boundary would increase the interference to adjacent cells, and consequently, would limit the radio link level throughput in those cells. Therefore, maximum allowable rates are allocated to the mobiles with the most favorable interference conditions (with respect to the other cells) in terms of peak-interference factor.

The rate-allocation procedure in this case can be described as follows.

1) Find the peak-interference factor $\hat{\eta}_{j'}(k) \triangleq \max_{j \neq j'} \{\eta_{j'/j}(k)\}$ corresponding to the kth mobile in cell j' (which characterizes peak interference to adjacent other cells $j \neq j'$ due to the kth mobile in cell j'), and repeat this for all $k = 1, \ldots, g_{j'}$ and $j' = 1, 2, \ldots, N_c$.
2) Allocate the maximum possible rate $m_i^{(j')}$ $(0 \le m_i^{(j')} \le \varphi)$ to the mobiles logically arranged in an increasing order of the corresponding peak interferences $\{\hat{\eta}_{j'}(k) \,|\, k = 1, \ldots, g_{j'};\, j' = 1, 2, \ldots, N_c\}$ to maximize throughput β.

C. Sum Interference-Based Dynamic Rate Adaptation

The idea behind this scheme is to minimize the composite of the other-cell interference, which is the sum of interferences generated by all the mobiles in a cell to the adjacent cells. In fact, the effect of spatial distribution of the mobiles on the joint multicell dynamic rate allocation may be more effectively taken into account through sum interference-based dynamic rate allocation. The joint multicell rate allocation, in this case, allocates the maximum allowable rate to the mobiles with the most favorable interference conditions (with respect to the other cells) in terms of the sum-interference factor, which is defined by $\tilde{\eta}_{j'}(k) \triangleq \sum_{j \neq j'} \eta_{j'/j}(k)$ for $k = 1, \ldots, g_{j'}$ and $j' = 1, 2, \ldots, N_c$.

VI. Radio Link Level Throughput

A. Analysis of Bit-Error Rate (BER) Under MDMC Signaling

Since the MDMC DS-CDMA is 2^m-ary $(1 \le m \le 8)$ bi-orthogonal signaling, a symbol-by-symbol detection yields the probability of symbol error, conditioned on γ_m as follows [11]:

$$p_{e,m}(\gamma_m) = 1 - \int_0^\infty [1 - 2Q(x)]^{2^{m-1}-1} \phi(x - \sqrt{2\gamma_m})\, dx \tag{26}$$

where $Q(x) = \int_x^\infty \phi(y)\, dy$ for $\phi(y) = 1/\sqrt{2\pi}\, e^{-y^2/2}$, and $\gamma_m \triangleq Z_i^{(j)}/2$ $(m = m_i^{(j)})$ has the probability density function [12]

$$f(\gamma_m) = \begin{cases} \frac{1}{(L-1)!\bar{\gamma}_{m,c}^L} \gamma_m^{L-1} \exp\left(-\frac{\gamma_m}{\bar{\gamma}_{m,c}}\right) \\ \quad \text{for equal average path power,} \\ \sum_{l=1}^{L} \frac{\pi_{m,l}}{\bar{\gamma}_{m,l}} \exp\left(-\frac{\gamma_m}{\bar{\gamma}_{m,l}}\right) \\ \text{for unequal average path power.} \end{cases} \tag{27}$$

[6]This optimality holds within the tagged cell or within a group of N_c cells, in the case of SINR Model-1 and SINR Model-2, respectively.

In the above, we have assumed that

$$\begin{aligned}\bar{\gamma}_{m,c} &= 1/2\,\mathbf{E}\{(\mathrm{SINR})_{o,i,l}^{(j)}\}|_{\sigma_l^2=1/L}\\ \sigma_l^2 &= \mathbf{E}\{a_{j,k(j'),l}^2\}\\ \bar{\gamma}_{m,l} &= 1/2\,\mathbf{E}\{(\mathrm{SINR})_{o,i,l}^{(j)}\}\\ \pi_{m,l} &= \prod_{\substack{l'=1\\ l'\neq l}}^{L} \bar{\gamma}_{m,l}/(\bar{\gamma}_{m,l}-\bar{\gamma}_{m,l'})\end{aligned}$$

where the per-path SINR is given by $(\mathrm{SINR})_{o,i,l}^{(j)} = a_{j,k(j),l}^2 (\mathrm{SINR})_{o,i}^{(j)}$ with respect to the RAKE-combined output SINR in (17) and (23). It is to be noted that the channel gain due to long-term fading $L_j(j',k)$ is assumed to be fixed during each rate-adaptation interval.

With the maximal ratio (independent) L-path coherent combining, the average probability of symbol error $p_{e,m}$ at rate v_m can be evaluated as in (28) below and (29) at the bottom of the page for the cases of equal average path power and unequal average path power, respectively, where $\Gamma(\cdot)$ is the gamma function and ${}_1F_1(\cdot,\cdot,\cdot)$ is the confluent hypergeometric function [13]

$$\begin{aligned}p_{e,m} =& \int_0^\infty p_{e,m}(\gamma_m) f(\gamma_m) d\gamma_m\\ =& 1-\int_o^\infty [1-2Q(x)]^{2^{m-1}-1}\left\{\frac{(2L-1)!}{(2)^{2L-1}(L-1)!}\right.\\ &\cdot \frac{e^- x^{2/2}}{(1+\bar{\gamma}_{m,c})^L}\\ &\cdot\left[\frac{1}{\sqrt{2}\Gamma\left(L+\frac{1}{2}\right)}{}_1F_1\left(L,\frac{1}{2},\frac{x^2}{2(1+\bar{\gamma}_{m,c}^{-1})}\right)\right.\\ &+\frac{x}{\Gamma(L)\sqrt{1+\bar{\gamma}_{m,c}^{-1}}}\\ &\left.\left.\cdot{}_1F_1\left(L+\frac{1}{2},\frac{3}{2},\frac{x^2}{2(1+\bar{\gamma}_{m,c}^{-1})}\right)\right]\right\}dx. \end{aligned} \tag{28}$$

Now, if we view the 2^m-ary bi-orthogonal signaling as a combination of antipodal and 2^{m-1}-ary orthogonal signaling, the BER can be well approximated to

$$p_{b,m} \cong \frac{2^{m-1}-1}{2^m-2}\, p_{e,m} \tag{30}$$

because errors may occur for antipodal signals with negligible probability. For instance, the QPSK with $m=2$ has the BER of $p_{b,m} \cong 1/2 p_{e,m}$.

B. BER Under VSF Signaling

In the case of L-path Rayleigh fading with equal average path power (which is referred to as Channel Model-A in this paper), $\bar{\gamma}_{m,c}$ is replaced by $\bar{\gamma}_c = 1/2\,\mathbf{E}\{(\mathrm{SINR})_{o,i,l}^{(j)}\}|_{\sigma_l^2=1/L}$, where the RAKE-combined output SINR is found in (21) and (24).

Let us denote by x the effective traffic load (i.e., $x \overset{\triangle}{=} \sum_{m=1}^{\varphi} mn_m$). Then, for maximal-ratio combining with independent L branches, the BER is given by [12]

$$p_b(x) = \left[\frac{1}{2}(1-\zeta)\right]^L \sum_{l=0}^{L-1}\binom{L-1+l}{l}\left[\frac{1}{2}(1+\zeta)\right]^l \tag{31}$$

where $\zeta = \sqrt{\bar{\gamma}_c/(1+\bar{\gamma}_c)}$.

In the case of multipath Rayleigh fading with unequal average path power (which is referred to as Channel Model-B in this paper), $\bar{\gamma}_{m,l}$ is replaced by $\bar{\gamma}_l = 1/2\,\mathbf{E}\{(\mathrm{SINR})_{o,i,l}^{(j)}\}$ with the RAKE-combined output SINR in (21) and (24). Then, the BER can be expressed by [12]

$$p_b(x) = \frac{1}{2}\sum_{l=1}^{L}\pi_l\left[1-\sqrt{\frac{\bar{\gamma}_l}{1+\bar{\gamma}_l}}\right] \tag{32}$$

where $\pi_l = \prod_{\substack{l'=1\\ l'\neq l}}^{L} \bar{\gamma}_l/(\bar{\gamma}_l-\bar{\gamma}_{l'})$.

The parameters for Channel Model-B in this paper are assumed to be based on the vehicular-B model [14] for macrocell.

C. Analysis of Radio Link Level Throughput

For the SR-based error control, a mobile with rate v_m can transmit up to m frames during a frame time, each containing N_f bits with t-bit error-correcting capability. Hence, for the SR-based error control

$$p_{c,m} = \sum_{i=0}^{t}\binom{N_f}{i} p_{b,m}^i (1-p_{b,m})^{N_f-i}. \tag{33}$$

With GBm-based error control, all the m frames transmitted during a frame time are considered a single frame of length mN_f bits with t_m-bit error-correcting capability, where t_m is chosen such that the code rate is the same as the single frame (with N_f bits) decoding case with t-bit error-correcting code. Hence, for the GBm-based error control

$$p_{c,m} = \sum_{i=0}^{t_m}\binom{mN_f}{i} p_{b,m}^i (1-p_{b,m})^{mN_f-i}. \tag{34}$$

In the case of VSF signaling, $p_{b,m}$ in (33) and (34) above would be replaced by $p_b(x)$ to yield $p_c(x)$. After $p_{c,m}$ ($p_c(x)$)

$$p_{e,m} = 1-\sum_{l=1}^{L}\int_0^\infty [1-2Q(x)]^{2^{m-1}-1}\left\{\frac{\pi_{m,l}e^{-x^2/2}}{\sqrt{2\pi}(1-\bar{\gamma}_{m,l})}+\frac{\pi_{m,l}x}{(1+\bar{\gamma}_{m,l}^{-1})}\exp\left[-\frac{x^2}{2(1+\bar{\gamma}_{m,l}^{-1})}\right]\left[1-Q\left(\frac{x}{\sqrt{1+\bar{\gamma}_{m,l}^{-1}}}\right)\right]\right\}dx \tag{29}$$

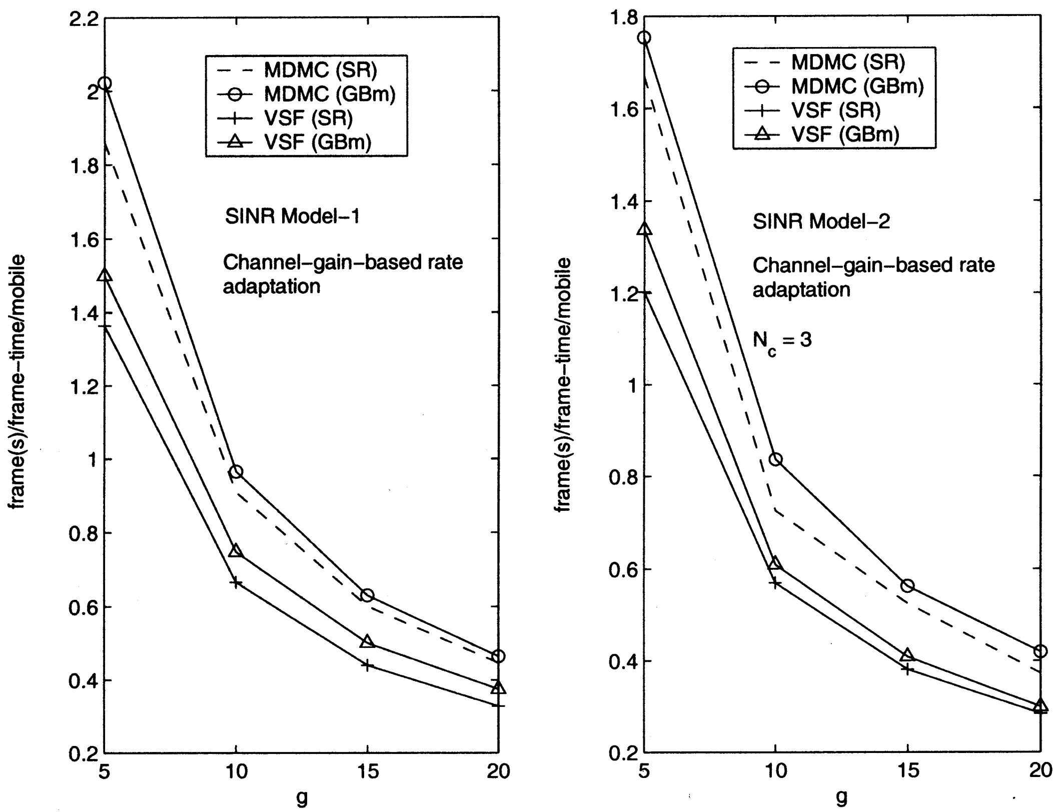

Fig. 3. Radio link level throughput comparison for MDMC and VSF signaling with channel gain-based dynamic rate adaptation (for Channel Model-B).

is determined, the radio link level throughput β can be evaluated by using (2).

In the case of joint N_c-cell rate adaptation under MDMC signaling, $p_{c,m}^{(j)}$ for the tagged cell j in (4) is evaluated through (30) and (33) or (34) by replacing $p_{e,m}$ with $p_{e,m}^{(j)}$. For VSF signaling, $p_c^{(j)}(x)$ is evaluated using (33) or (34) with $p_{b,m}$ replaced by $p_b^{(j)}(x)$ as determined through (31) or (32).

D. Numerical Results and Discussions

Radio link level throughput (β) is evaluated under dynamic rate adaptation with MDMC and VSF signaling for both the SR- and the GBm-based error control schemes using SINR Model-1 and SINR Model-2 (i.e., for single-cell and joint multicell rate adaptation, respectively) (Figs. 3–5). The assumed values for some of the simulation parameters are provided in Table II. The long-term fading in (20) is assumed to be constant over a frame time T_f. The values of $\rho_j(j', k)$ and $\rho_{j'}(j', k)$, which account for the short-term fading in (19), are assumed to be constant only over a fraction of the frame-time Δt, where $T_f = N_s \Delta t$ (e.g., $N_s =$ number of power control slots per frame time).[7] Therefore, the value of $\eta_{j'/j}(k)$ over a frame time is calculated by using the average of the N_s independent values of $\rho_j(j', k)/\rho_{j'}(j', k)$.

As is evident from Figs. 3–5, for all of the rate-adaptation algorithms, higher throughput performance is achieved with MDMC signaling over a range of system load g for both the SR- and the GBm-based error control schemes. This observation holds for both SINR Model-1 and SINR Model-2 (i.e, for both single cell and joint multicell rate adaptation). This is due to the higher SINR achieved for MDMC signaling at the cost of receiver complexity. Since in a time-dispersive environment the performance of the conventional MC transmission is similar to the performance of VSF transmission [3], similar observations can be made when comparing the performances of MDMC signaling and conventional MC transmission.

The performance comparison among the different heuristic-based rate-adaptation algorithms with MDMC signaling under joint multicell rate adaptation is illustrated in Fig. 6. The channel gain-based dynamic rate adaptation is observed to perform consistently better compared to the other schemes under both MDMC and VSF signaling.

With mean-sense approximation for the other-cell interference (i.e., with SINR Model-1), the effect of the other-cell interference on the tagged cell is rather optimistic, and for this reason, the average throughput per mobile per frame time is observed to be higher, compared with that obtainable for SINR Model-2 with all the heuristic-based rate-adaptation algorithms presented in this paper. With SINR Model-1, the performance difference among the channel gain-based, the peak interference-based, and the sum interference-based rate adaptation is observed to be not significant at all (as speculated in Section IV-D).

With optimal dynamic rate adaptation (which is determined by an exhaustive search among all possible rate allocations to $\sum_{j=1}^{N_c} g_j$ mobiles in N_c cells), based on some of our earlier experiments (as reported in [6]), we expect that the performance improvement is not significantly better than that achievable with channel gain-based or sum interference-based rate allocation.

[7]The value of N_s is assumed to be 16 in this paper.

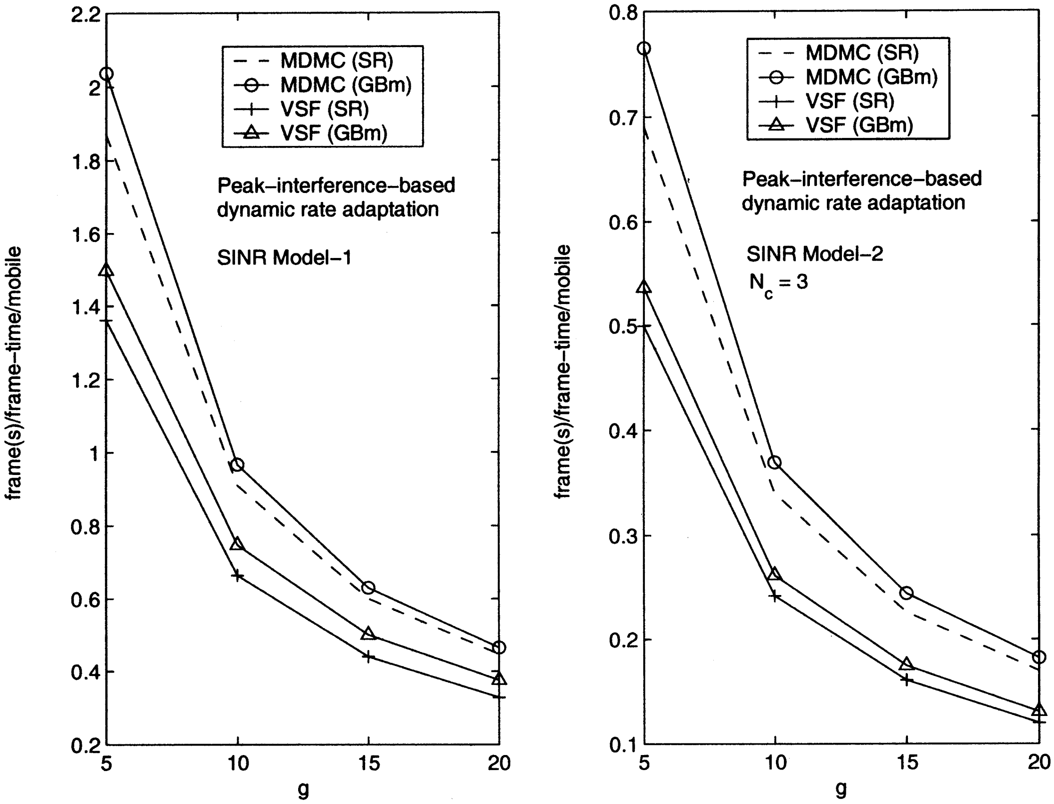

Fig. 4. Radio link level throughput comparison for MDMC and VSF signaling with peak interference-based dynamic rate adaptation (for Channel Model-B).

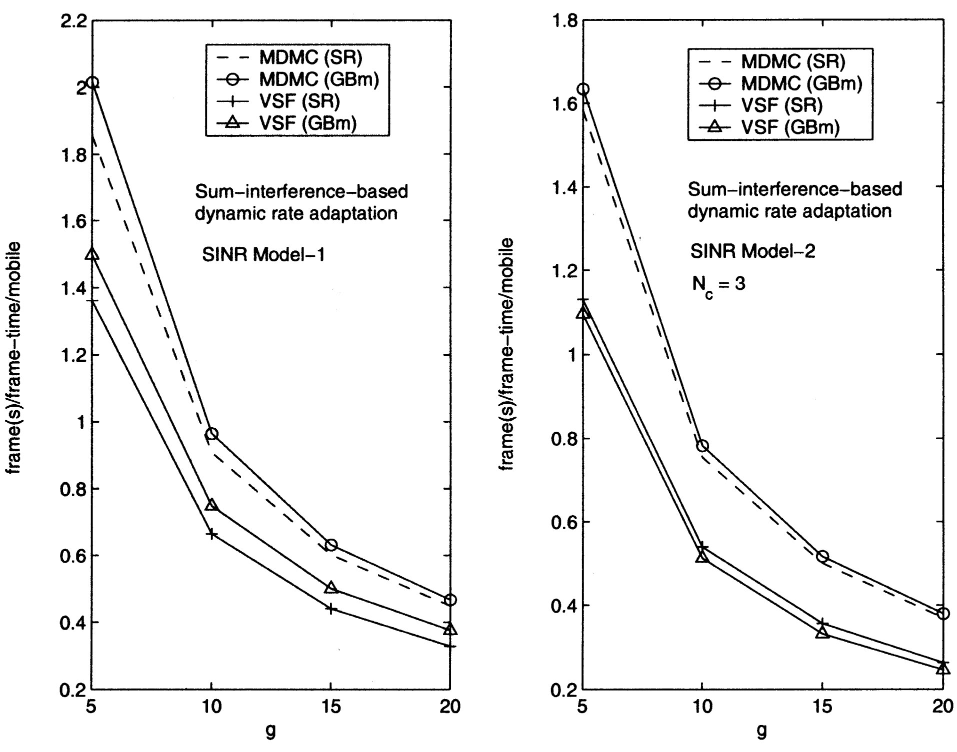

Fig. 5. Radio link level throughput comparison for MDMC and VSF signaling with sum interference-based dynamic rate adaptation (for Channel Model-B).

VII. BS-Assisted and Mobile-Controlled Rate Adaptation

In a BS-controlled (i.e., centralized) dynamic rate and error-control scheme, the BS dynamically assigns the transmission rates to the mobiles based on the traffic load and the channel condition. The transmission rate assignment may be based on the single-cell dynamic rate adaptation or joint multicell rate adaptation as discussed earlier in this paper. But in any case, it

TABLE II
SIMULATION PARAMETERS

Parameter	Value
Frame-time, T_f	10 ms
Chip sequence length, N	128
Frame length, N_f	128 bits
No. of cells, J	19
Path-loss exponent, δ	4.0
Standard deviation of shadow fading, σ	8 dB
Maximum normalized transmission rate, φ	8
No. of parallel code channels, M	4
FEC parameter, t	2
No. of resolvable multipaths, L for channel model-A (model-B)	4 (6)
E_b/N_0, dB	10
No. of power control slots/frame	16

requires the BSs to know in advance the corresponding interference factors (or in other words, the exact number of users ready to transmit and their channel conditions during a frame time). Information regarding the number of ready-to-transmit users can be conveyed either by some preamble bits (as in the BS-II Algorithm in [15]) or by the subrate channel maintained for each connection. Either of these schemes may cause a loss in the effective radio channel utilization.

In another type of centralized implementation, the BS can assign the transmission rates based on an estimate of the number of ready-to-transmit users $\{g_j\}$ during a frame time rather than the exact number of users that will transmit during the next frame time (e.g., BS-I Algorithm in [15]). Channel load estimation under a bursty traffic environment may not be simple and it may lead to some *ad hoc* rate-adaptation algorithm.

In fully distributed dynamic rate adaptation, each mobile can choose a transmission rate independently; the problem here is to determine proper adaptation criteria and a suitable method of rate adaptation. Hybrid schemes can be devised for uplink packet data transmission where the BS can assist the mobiles in performing the dynamic rate adaptation. Such a hybrid BS-assisted mobile-controlled dynamic rate adaptation algorithm is proposed in this paper.

In the proposed scheme, each mobile initially chooses an appropriate transmission rate among the permissible transmission rates. Each mobile updates its transmission rate based on its transmission status. It increases the rate in the case of successful transmission, while it decreases the rate in the case of transmission failure.

If any one of the frames (all of the frames) transmitted by a mobile with rate v_m is (are) correctly received in the case of SR-(GBm-) based error control, let the probability that the mobile increases the rate to v_{m+1} in the next transmission attempt be p_s. If all the frames are in error, let the probability that the mobile decreases the rate to v_{m-1} in the next transmission attempt be p_f. Based on the feedback information on transmission status, each mobile updates the values of p_s and p_f locally during each frame time. In addition to that, the parameters p_s and p_f are updated periodically based on the information broadcast by the BS. This enables the mobiles to exploit some global information for dynamic rate adaptation. Therefore, the rate adaptation algorithm can be viewed as a BS-assisted and mobile-controlled (distributed) algorithm.

The BS estimates the offered load $g = \mathbf{E}[g_j]$ and the average number of active users $\bar{n}_m = \mathbf{E}[n_m]$ using rate v_m, $m = 0, 1, \ldots, \varphi$ over a certain time window (W), which is comprised of several transmission frame times. Based on these estimates, the values of p_s and p_f can be determined and can be periodically broadcast by the BS using a control channel. The mobiles use these estimated values of p_s and p_f as the initial values for transmission during the next time window.

The estimation of p_s and p_f from the average load and the transmission-rate information (which is based on equilibrium point analysis [16] of the system in steady state as will be presented later) is such that the value of p_s (p_f) is increased (reduced) when the system load is low, and the value of p_s (p_f) is reduced (increased) when the system load is high. The system load during a time window of measurement is reflected in the number of transmission attempts and the corresponding rates chosen by the different mobile users.

Since only the average load information, rather than the actual instantaneous traffic load information, is used to estimate p_s and p_f, and the local adaptation of the parameters p_s and p_f is heuristic based, the performance of such a scheme would be inferior to that of the ideal dynamic rate adaptation.[8] On the other hand, such a scheme may offer the advantage of implementation simplicity.

If K is the number of active users in a desired cell, then $K = \sum_{m=0}^{\varphi} k_m$, where k_m is the number of mobiles with rate v_m at a certain time. Note that under the assumption of binomial distribution on frame transmission with parameters (K, p), K equals gp^{-1}.

Suppose that the system is at an equilibrium point. Then, considering the rates v_{m-1}, v_m, and v_{m+1}, the set of balance equations in (35) can be obtained, where $p_{c,m}$ depends on the error control scheme (i.e., SR or GBm) employed and $p_{c,0} = 1$

$$\begin{aligned} k_0(p_{c,0}P_s) &= k_1(1 - p_{c,1})p_f, m = 0 \\ k_m(p_{c,m}p_s) + k_m(1 - p_{c,m})p_f &= km - 1(p_{c,m-1}P_s) \\ &\quad + k_{m+1}(1 - p_{c,m+1})p_f, \\ &\quad 1 \leq m \leq \varphi - 1 \\ k_{\varphi-1}(p_{c,\varphi-1}p_s) &= k_\varphi(1 - p_{c,\varphi})p_f, m = \varphi. \end{aligned} \tag{35}$$

Solving the above equations, we obtain

$$k_m = k_0 \prod_{l=0}^{m-1} \frac{p_{c,l}}{1 - p_{c,l+1}} \left(\frac{p_s}{p_f}\right)^m, \qquad m = 1, 2, \ldots, \varphi. \tag{36}$$

[8]The ideal case refers to when the BS knows exactly the number of ready-to-transmit mobiles.

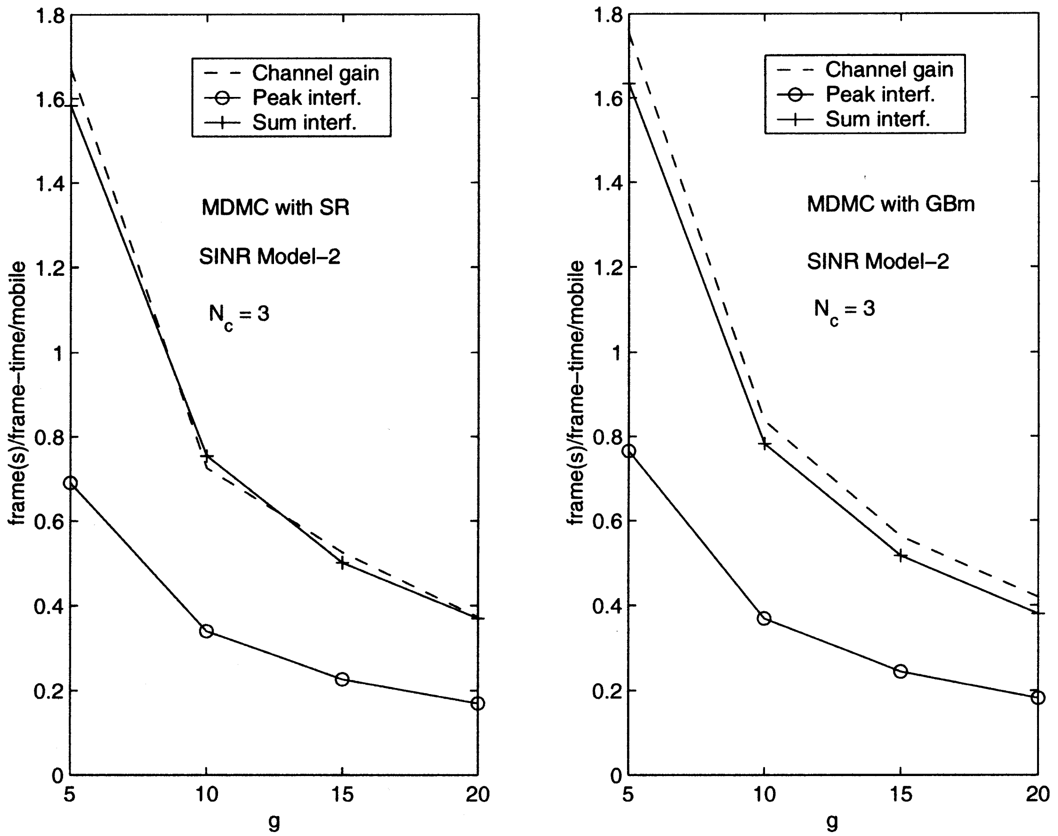

Fig. 6. Radio link level throughput comparison for the different heuristic-based rate adaptation algorithms (for MDMC signaling and Channel Model-B).

Using the constraint $\sum_{m=0}^{\varphi} k_m = gp^{-1}$

$$\frac{g}{\bar{n}_0} = 1 + \sum_{m=1}^{\varphi} a_m x^m \text{ or } \frac{g}{\bar{n}_m} a_m x^m = 1 + \sum_{m=1}^{\varphi} a_m x^m \quad (37)$$

where $\bar{n}_m = k_m p$, $a_0 = 1$, $a_m = \prod_{l=0}^{m-1} p_{c,l}/(1 - p_{c,l+1})$ ($m \geq 1$), and $x \stackrel{\triangle}{=} p_s/p_f$.

It is interesting to note that, if $\bar{n}_0 = g$, namely, all mobiles use the rate zero for transmissions, then we have $x = 0$. This implies that $p_s = 0$ for a nonzero p_f, and hence, $k_0 = K$. On the other hand, $p_s \rightarrow 1$ as $\bar{n}_0 \rightarrow 0$. These are intuitively satisfying. Therefore, based on (37), an efficient dynamic adaptation of x (and hence, p_s and p_f) can be achieved. The value of x is estimated as the average of the values of x, which are evaluated by using each of the measured values of $\bar{n}_m$ ($0 \leq m \leq \varphi$) in (37).

Now, based on the load and rate estimations and the relation in (37), an iterative method for global adaptation of the values (p_s, p_f) is proposed as follows.

1) The BS estimates $g(t-1)$ and $\{\bar{n}_m(t-1)\}$ (average number of users using the rate v_m during a frame time) over the $(t-1)$th time window, where the estimates are allowed to be noninteger values [16]. These estimates are used to update the values of p_s and p_f for the tth time window.
2) Using the estimates, determine $x(t)$ that satisfies (37) where $\{a_m\}$, which is a function of $\{p_{c,m}\}$, depends on $\{\bar{n}_m(t-1)\}$ through $(\mathrm{SINR})_{o,i}^{(j)}$ in (17) with $\sum_{k=1}^{g_j} m_k^{(j)} \rightarrow \sum_{m=1}^{\varphi} m\bar{n}_m(t-1)$ and $\bar{\eta}_j \rightarrow \bar{\eta} = \mathbf{E}[\bar{\eta}_j]$.
3) Update the values $p_s(t-1)$ and $p_f(t-1)$ as follows: $p_s(t) = p_s(t-1) + \Delta(t)$ and $p_f(t) = p_f(t-1) - \Delta(t)$ (with the constraint $0 \leq p_s, p_f \leq 1.0$), where the step size $\Delta(t)$ is determined by using the following relation:

$$\frac{p_s(t-1) + \Delta(t)}{p_f(t-1) - \Delta(t)} = x(t). \quad (38)$$

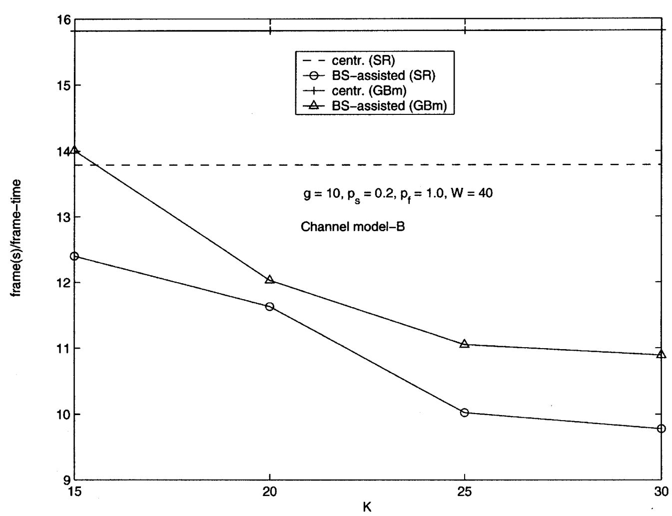

Fig. 7. Throughput performance with BS-assisted mobile-controlled dynamic rate adaptation (with MDMC signaling).

In addition, each mobile updates the value of p_s (p_f) locally within the time window according to an additive increase and multiplicative decrease (AIMD) method [17].

With the AIMD method, for successful transmission of at least one frame (all frames) in the case of SR- (GBm-) based error control, the values of p_s and p_f are updated as follows: $p_s^{(t)}(i+1) = p_s^{(t)}(i) + (1 - p_s^{(t)}(i)) \times a$ and $p_f^{(t)}(i+1) = p_f^{(t)}(i) \times b$, where $0.0 < a < 1.0$, $0.0 < b \leq 1.0$. Here, $p_s^{(t)}(i)$ ($p_f^{(t)}(i)$) and $p_s^{(t)}(i+1)$ ($p_f^{(t)}(i+1)$) are the values of p_s (p_f) at the ith and $(i+1)$th frame time, respectively, during the tth window period.

In the case of transmission failure (i.e., when all of the frames transmitted during a frame time are unsuccessful), the values of p_s and p_f are updated as follows: $p_s^{(t)}(i+1) = p_s^{(t)}(i) \times b$ and $p_f^{(t)}(i+1) = p_f^{(t)}(i) + (1 - p_f^{(t)}(i)) \times a$.

The above steps are repeated for each time window. The window size (W) and the local adaptation parameters (i.e., a, b) may be suitably adjusted to achieve a high throughput β.

Typical performance results are illustrated in Fig. 7 for both the SR- and the GBm-based error control. It is assumed that the BS estimates g and $\bar{n}_m$ based on the number of correctly received frames. The performance results in the case of channel gain-based centralized rate adaptation with fixed channel load $g = 10$ [shown as centr. (SR) and centr. (GBm)] are also presented for performance comparison. The performance results indicate that the proposed rate-adaptation scheme has the potential of reasonably high performance when the protocol parameters are properly chosen.

VIII. Conclusion

The performance of MDMC signaling, as a means of achieving variable-rate uplink packet data transmission in cellular WCDMA networks, has been modeled and analyzed. The MDMC signaling offers higher link level throughput compared to the other methods for achieving variable-rate transmission (e.g., VSF transmission and conventional MC transmission). Among the three heuristic-based rate-adaptation schemes, the channel gain-based rate adaptation offers the best throughput performance in the case of both single cell and joint multicell rate adaptation. The presented analytical framework enables us to evaluate the effects of the propagation parameters (e.g., path loss exponent, shadowing parameter) and the other channel parameters on the link level throughput, and hence, on higher layer (e.g., transmission control protocol) throughput in a variable-rate transmission scenario in a cellular WCDMA network. The performance of the proposed BS-assisted and mobile-controlled dynamic rate-adaptation procedure has been observed to be reasonably close to the performance of the ideal suboptimal centralized rate-adaptation policy.

References

[1] C.-L. I and R. D. Gitlin, "Multicode CDMA wireless personal communications networks," in *Proc. IEEE ICC '95*, 1995, pp. 1060–1063.

[2] C.-L I and K. K. Sabnani, "Variable spreading gain with adaptive control for true packet switching wireless network," in *Proc. IEEE ICC '95*, 1995, pp. 725–730.

[3] E. Dahlman and K. Jamal, "Wideband services in a DS-CDMA based FPLMTS system," in *Proc. IEEE VTC '96*, 1996, pp. 1656–1660.

[4] D. I. Kim and V. K. Bhargava, "Performance of multidimensional multicode DS-CDMA using code diversity and error detection," *IEEE Trans. Commun.*, vol. 49, pp. 875–887, May 2001.

[5] R. V. Nobelen, N. Seshadri, J. Whitehead, and S. Timiri, "An adaptive radio link protocol with enhanced data rates for GSM evolution," *IEEE Pers. Commun. Mag.*, vol. 6, pp. 54–64, Feb. 1999.

[6] D. I. Kim, E. Hossain, and V. K. Bhargava, "Dynamic rate adaptation and integrated rate and error control in cellular WCDMA networks," *IEEE Trans. Wireless Commun.*, submitted for publication.

[7] E. Dahlman *et al.*, "UMTS/IMT-2000 based on wideband CDMA," *IEEE Commun. Mag.*, vol. 36, pp. 70–80, Sept. 1998.

[8] S. Sasaki, H. Kikuchi, J. Zhu, and G. Marubayashi, "Multiple-access performance of parallel combinatory spread spectrum communication systems in nonfading and Rayleigh fading channels," *IEICE Trans. Commun.*, vol. E78-B, pp. 1152–1161, Aug. 1995.

[9] M. B. Pursley, "Performance evaluation for phase-coded spread-spectrum multiple-access communication—Part I: System analysis," *IEEE Trans. Commun.*, vol. COM-25, pp. 795–799, Aug. 1977.

[10] K. S. Gilhousen *et al.*, "On the capacity of a cellular CDMA system," *IEEE Trans. Veh. Technol.*, vol. 4, pp. 303–312, May 1991.

[11] J. M. Wozencraft and I. M. Jacobs, *Principles of Communication Engineering*. New York: Wiley, 1965.

[12] J. G. Proakis, *Digital Communications*, 2nd ed. New York: McGraw-Hill, 1989.

[13] *Handbook of Mathematical Functions*, M. Abramowitz and I. A. Stegun, Eds., National Bureau of Standards, Washington, DC, 1964.

[14] "Guidelines for Evaluation of Radio Transmission Technologies for IMT-2000,", Rec. ITU-R M.1225, 1997.

[15] O. Sallent and R. Agustí, "A proposal for an adaptive S-ALOHA access system for a mobile CDMA environment," *IEEE Trans. Veh. Technol.*, vol. 47, pp. 977–985, Aug. 1998.

[16] S. Tasaka, *Performance Analysis of Multiple Access Protocols*. Cambridge, MA: MIT Press, 1986.

[17] R. Jain, K. Ramakrishnan, and D. Chiu, "Congestion avoidance in computer networks with a connectionless network layer," in *Innovations in Internetworking*, C. Partridge, Ed. Norwood, MA: Artech House, 1988.

Dong In Kim (S'89–M'90–SM'02) received the B.S. and M.S. degrees in electronics engineering from Seoul National University, Seoul, Korea, in 1980 and 1984, respectively, and the M.S. and Ph.D. degrees in electrical engineering from University of Southern California (USC), Los Angeles, in 1987 and 1990, respectively.

From 1984 to 1985, he was with the Korea Telecom Research Center as a Researcher. During 1986–1988, he was a Korean Government Graduate Fellow in the Department of Electrical Engineering, USC. From 1991 to 2002, he was with the University of Seoul, Seoul, Korea, leading the Wireless Communications Research Group. He is currently with Simon Fraser University, Burnaby, BC, Canada, where he is an Associate Professor of the School of Engineering Science. He was a Visiting Professor at University of Victoria, Victoria, BC, Canada, during 1999–2000. He has performed research in the areas of packet radio networks and spread-spectrum systems since 1988. His current research interests include spread-spectrum systems, cellular mobile communications, indoor wireless communications, and wireless multimedia networks.

Dr. Kim has served as an Editor for the IEEE Journal on Selected Areas in Communications: Wireless Communications and also as a Division Editor for the *Journal of Communications and Networks*. Currently, he serves as an Editor for the IEEE Transactions on Communications and the IEEE Transactions on Wireless Communications.

Ekram Hossain (S'98–M'00) received the Ph.D. degree in electrical engineering from the University of Victoria, Victoria, BC, Canada, in 2000, and the B.Sc. and M.Sc. degrees, both in computer science and engineering from Bangladesh University of Engineering and Technology (BUET), Dhaka, Bangladesh, in 1995 and 1997, respectively.

He is currently an Assistant Professor in the Department of Electrical and Computer Engineering, University of Manitoba, Winnipeg, MB, Canada. His main research interests include radio link control and transport layer protocol design issues for the next-generation wireless data networks.

Dr. Hossain was a University of Victoria Fellow, and currently he serves as an Editor for the IEEE TRANSACTIONS ON WIRELESS COMMUNICATIONS.

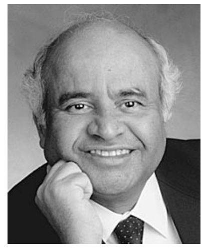

Vijay K. Bhargava (S'70–M'74–SM'82–F'92) received the B.Sc., M.Sc., and Ph.D. degrees from Queen's University, Kingston, ON, Canada in 1970, 1972, and 1974, respectively.

Currently, he is a Professor of Electrical and Computer Engineering at the University of Victoria, Victoria, BC, Canada, and holds a Canada Research Chair in Wireless Communications. He is a co-author of the book *Digital Communications by Satellite* (New York: Wiley, 1981) and co-editor of the book *Reed–Solomon Codes and Their Applications* (Piscataway, NJ: IEEE Press). His research interests are in multimedia wireless communications.

Dr. Bhargava is a Fellow of the British Columbia Advanced Systems Institute, the Engineering Institute of Canada (EIC), the Canadian Academy of Engineering, and the Royal Society of Canada. He is a recipient of the IEEE Centennial Medal (1984), IEEE Canada's McNaughton Gold Medal (1995), the IEEE Haraden Pratt Award (1999), the IEEE Third Millennium Medal (2000), and the IEEE Graduate Teaching Award (2002). Currently he serves on the Boards of the IEEE Information Theory and Communications Societies, and is a Past President of the IEEE Information Theory Society. He is an Editor for the IEEE TRANSACTIONS ON COMMUNICATIONS and the IEEE TRANSACTIONS ON WIRELESS COMMUNICATIONS.